DOI 10.1007/s10946-024-10202-9
Journal of Russian Laser Research, Volume 45, Number 2, March, 2024

CONTINUOUS-WAVE LASING CHARACTERISTICS OF Ho : $GdVO_4$ CRYSTAL UNDER DIODE-PUMPING ARCHITECTURE

Jiaze Wu,[1] Xiaoming Duan,[1,2*] Yu Ding,[3] Wensheng Zhang,[4] Jihe Yuan,[5] and Zuochun Shen[1]

[1] *National Key Laboratory of Tunable Laser Technology, Harbin Institute of Technology Harbin 150001, China*

[2] *Zhengzhou Research Institute of Harbin Institute of Technology Zhengzhou 450000, China*

[3] *National Key Laboratory of Electromagnetic Space Security Tianjin 300308, China*

[4] *Department of physics, Harbin University Harbin 150086, China*

[5] *College of Physical Science and Technology, Heilongjiang University Harbin 150080, China*

*Corresponding author e-mail: xmduan@hit.edu.cn; szc@hit.edu.cn

Abstract

In this paper, we investigate the continuous-wave lasing characteristics of Ho : $GdVO_4$ crystal under diode-pumping conditions. Using a 1.0 at.%-doped crystal, we obtain the maximum output power equal to 9.0 W at 2047.9 nm, with an absorbed pump power of 28.2 W. The slope efficiency and optical efficiency measured with respect to the absorbed pump power are 50.7% and 31.9%, respectively. In addition, we estimate the beam quality factor at the maximum output level to be about 1.8.

Keywords: diode-pumped lasers, continuous-wave regime, Ho : $GdVO_4$.

1. Introduction

All solid-state Ho lasers operating at 2 μm are attractive for many technical applications, such as remote sensing, environment monitoring, plastic welding, medicine, and nonlinear optical conversion [1–5]. Commonly, the laser emitting at 1.9 μm is a good choice to pump the Ho medium because of the low quantum defect between the pump and lasing photons. Under high-performance diode-pumped Tm-laser pumping, the continuous-wave (CW) and Q-switched characteristics of the Ho crystal have been widely investigated [6–15]. But this approach (diode-Tm-Ho) is relatively complex, leading to the low overall conversion efficiency of the whole Ho-laser system. A solution is the directly diode-pumping method (diode-Ho). Ho-doped garnets and fluorides are often used in the diode-pumped architecture [16–25].

Compared with garnets and fluorides, the Ho-doped gadolinium vanadate (Ho : $GdVO_4$) crystal has high thermal conductivity. In addition, it also has a large emission cross-section, which benefits generating a high-efficiency laser output at 2 μm. Using Tm-laser as the pump source, we investigate the lasing

Manuscript submitted by the authors in English on February 11, 2024.

characteristics of Ho : $GdVO_4$ crystal [26–30]. However, there is not too many publications on the lasing characteristics of Ho : $GdVO_4$ crystal under diode-pumping conditions. In 2021, a CW maximum output power of 1.8 W at 2.05 μm was demonstrated in a diode-pumped Ho : $GdVO_4$ laser [31]. In 2022, the acousto-optically Q-switching performance of the diode-pumped Ho : $GdVO_4$ laser was reported with a repetition rate of 5 kHz and a pulse energy of 1.3 mJ [32]. In 2023, the electro-optically Q-switched diode-pumped Ho : $GdVO_4$ laser reached a pulse energy of 3.25 mJ at a repetition rate of 1 kHz [33]. Although several Watts of CW output were achieved in [32, 33]l nevertheless, the CW lasing characteristics of Ho : $GdVO_4$ crystal need to be further studied in detail.

In this work, we investigate the CW lasing characteristics of the Ho : $GdVO_4$ crystal with diode-pumping architecture. We achieve a maximum output power of 9.0 W with an absorbed pump power of 28.2 W, corresponding to a slope efficiency of 50.7% with respect to the absorbed pump power and an optical efficiency of 31.9%. In addition, we estimate the beam quality factor M^2 at the maximum output level to be about 1.8.

2. Experimental Setup

In Fig. 1, we present the experimental setup of a diode-pumped Ho : $GdVO_4$ laser. A dual-end-pumping architecture is used in this experiment. The Ho : $GdVO_4$ crystal with a doped concentration of 1.0 at.% is grown by the Czochralski method; it is cut along the a-axis with dimensions of 3×3×20 mm (length). Two end faces of the crystal are coated to be anti-reflected for the pump and lasing wavelengths. A water-cooled heat sink and a 0.1 mm thick Indium foil are used to wrap the laser crystal. The operating temperature of the heat sink is controlled at 18°C with an accuracy of 0.2°C.

Two fiber-coupled diodes (Dilas Corp., Multi-Bar Module) with a core diameter of 600 μm and a numerical aperture of 0.22 are used as the pump source. Each diode can produce 20 W output power at 1.94 μm. The output spectrum of the LD is monitored by an optical spectral analyzer (Bristol 721A). At the maximum output level, the central wavelength is located at 1939 nm with a full width at half maximum line width of about 9 nm. In addition, nearly 7 nm wavelength-shift is recorded, when the diode power increases from the threshold to the maximum. A power meter (Coherent PM30) is used to record the output powers. The absorption efficiency of Ho : $GdVO_4$ crystal is measured under non-lasing

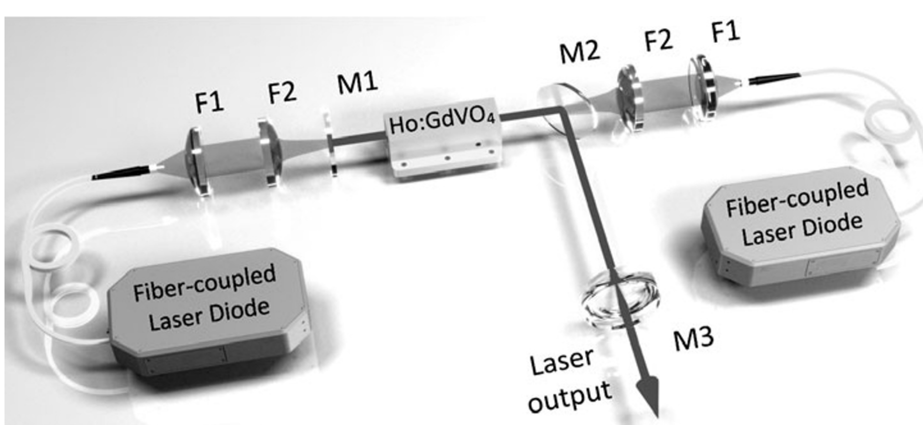

Fig. 1. The experimental setup of CW diode-pumped Ho : $GdVO_4$ laser.

conditions, indicating a variation of 64%−75% with increase in the diode power from the threshold to the maximum.

The pump beam diameter is set at be about 0.6 mm being transformed by lenses F1 and F2 with a focal length of 25 mm. The laser cavity consists of a 0°C flat mirror M1, a 45° flat mirror M2, and a plano-concave mirror M3. The M1 and M2 are coated with a high transmission at 1.94 μm and a high reflection at 2.05 μm. The M3 is an output coupler coated with a partial reflection for lasing wavelength. The whole cavity has a 100 mm physical length.

3. Experimental Results and Discussion

In Fig. 2, we present the CW output characteristics of the dual-end-pumped Ho : $GdVO_4$ laser under study; here, we see the output powers at the curvature radius of M3 equal to 300 mm (a) and 500 mm (b) and the relationship between the absorbed pump power and the output power at different transmittances of M3.

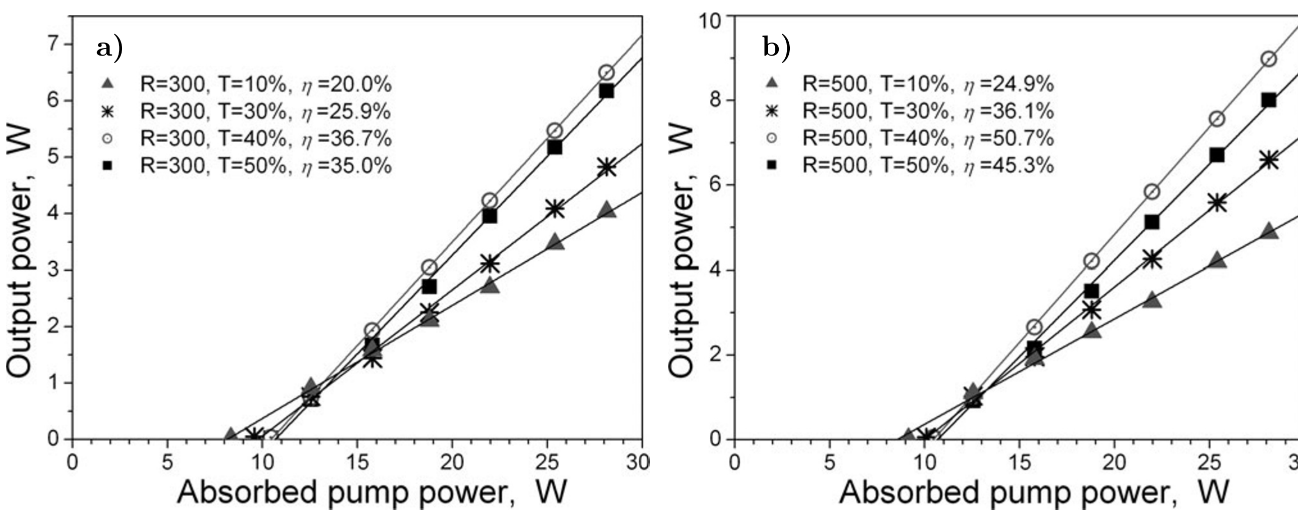

Fig. 2. The output characteristics of diode-pumped Ho : $GdVO_4$ laser; here, we see the output powers at the curvature radius of M3 equal to 300 mm (a) and 500 mm (b) and the relationship between the absorbed pump power and the output power when the transmittances of M3 are equal to 10% (▲), 30% (⋇), 40% (⊙), and 50% (■).

When the curvature radius of M3 is equal to 300 mm, a maximum output power of 6.5 W is obtained with a transmittance of 40% and an absorbed pump power of 28.2 W, corresponding to a slope efficiency of 36.7% with respect to the absorbed pump power and an optical efficiency of 23.1%; the pump threshold is equal to 10.5 W. When the transmittances of M3 are 50%, 30%, and 10%, the output powers are 6.2, 4.8, and 4 W, corresponding to slope efficiencies of 35%, 25.9%, and 20% and optical efficiencies of 22%, 17.2%, and 14.4%, respectively. One can see that the slope efficiency and the output power do not linearly increase with increase in the transmittance of mirror M3; there exists an optimum output transmittance of the Ho : $GdVO_4$ laser.

Afterwards, we change the curvature radius of mirror M3 to be equal to 500 mm and find that the overall output performance of the laser is improved; see Fig. 2 b. The highest slope efficiency with respect to the absorbed pump power of up to 50.7% is obtained at the transmittance of M3 to be equal to 40%;

the highest output power is 9.0 W and the optical efficiency is calculated to be about 31.9%. When the transmittances of M3 are 50%, 30%, and 10%, the output powers are 8.0, 6.6, and 4.9 W, corresponding to slope efficiencies of 45.3%, 36.1%, and 24.9% and optical efficiencies of 28.5%, 23.5%, and 17.3%, respectively. The output characteristics of diode-pumped $Ho:GdVO_4$ laser under two different curvature radii present similar trends, both reach the highest output level, when the transmittance of mirror M3 is 40%. Furthermore, as the transmittance of mirror M3 decreases, the pump threshold decreases. This is a normal phenomenon, because the low transmittance makes it easier to reach the upper-level particle population inversion condition in the laser cavity and form the laser oscillation. Nevertheless, in Fig. 2, one can see that the absorbed pump power and output power show a good linear relationship whether the output coupler M3 changes. No obvious power saturation phenomenon is measured. We believe that the output power could be improved with increasing pump power.

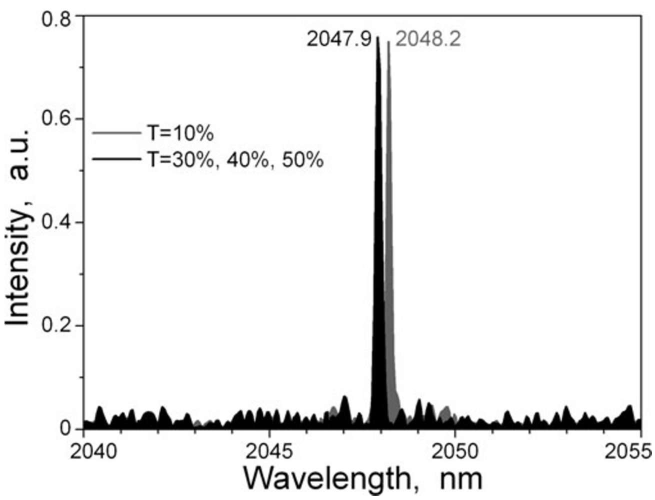

Fig. 3. Output spectra of the CW diode-pumped $Ho:GdVO_4$ laser.

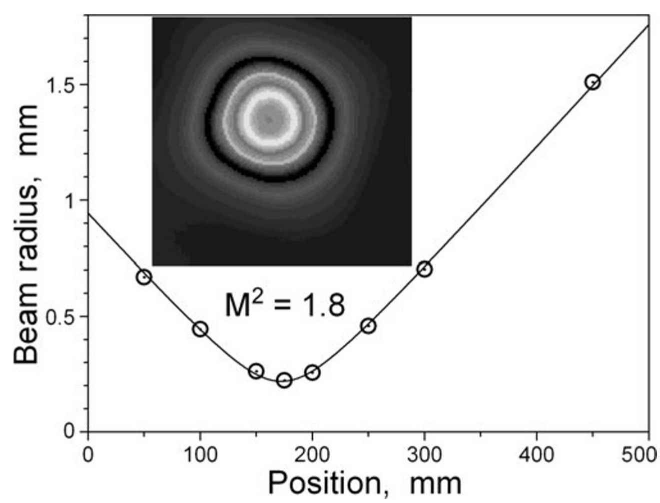

Fig. 4. The M^2 measurement of CW diode-pumped $Ho:GdVO_4$ laser.

We measure the output spectra of the CW diode-pumped $Ho:GdVO_4$ laser with transmittances of 10%, 30%, 40%, and 50%; see Fig. 3. When the output transmittance is 10%, the central wavelength is 2048.2 nm; in addition, the central wavelength is located at 2047.9 nm, and no obvious wavelength-shift is measured with increasing pump power. With the maximum output level, the M^2 factor is measured by the 90/10 knife-edge method. A lens with a focal length of 150 mm is used to transform the laser beam. The beam radii along the beam propagation direction are presented in Fig. 4. The M^2-factor is estimated to be about 1.8. In addition, we show a 2D picture of the far-field beam taken by a camera (Spiricon IV); see the insert in Fig. 4.

4. Summary

In conclusion, in the study, we investigated the CW output characteristics of $Ho:GdVO_4$ laser dual-end-pumped by two fiber-coupled diodes at 1.94 μm. The highest output power of up to 9.0 W was achieved with an absorbed pump power of 28.2 W. The slope efficiency and optical efficiency measured with respect to the absorbed pump power were 50.7% and 31.9%, respectively. In addition, the M^2 factor at the maximum output level was estimated to be about 1.8. The experimental results indicate that the diode-pumped Ho : $GdVO_4$ laser is a candidate for a compact efficient all solid-state 2 μm laser.

References

1. T. J. Wagener, N. Demma, J. D. Kmetec, and T. S. Kubo, *IEEE Aerosp. Electron. Syst. Mag.*, **10**, 23 (1995).
2. A. Pal, R. Sen, K. Bremer, et al., *Appl. Opt.*, **51**, 7011 (2012).
3. I. Mingareev, F. Weirauch, A. Olowinsky, et al., *Opt. Laser Technol.*, **44**, 2095 (2012).
4. M. S. Kopyeva, S. A. Filatova, V. A. Kamynin, et al., *Photonics*, **9**, 20 (2022).
5. X. Duan, L. Li, Y. Shen, et al., *Appl. Opt.*, **57**, 8102 (2018).
6. J. W. Zhang, F. Schulze, K. F. Mak, et al., *Laser Photonics Rev.*, **12**, 1700273 (2018).
7. W. Koen, C. Bollig, H. Strauss, et al., *Appl. Phys. B*, **99**, 101 (2010).
8. X. M. Duan, B. Q. Yao, X. T. Yang, et al., *Opt. Express*, **17**, 4427 (2019).
9. V. Jambunathan, X. Mateos, P. A. Loiko, et al., *J. Lumin.*, **179**, 50 (2016).
10. M. Jelínek, V. Kubecek, W. Ma, et al., *Laser Phys. Lett.*, **13**, 065004 (2016).
11. Q. Wang, Q. Long, Y. Gao, et al., *Appl. Opt.*, **60**, 8046 (2021).
12. L. Guo, S. Zhao, T. Li, et al., *Opt. Laser Technol.*, **126**, 106015 (2020).
13. W. Weng, H. Huang, H. Wu, et al., *Opt. Commun.*, **532**, 129248 (2023).
14. X. Duan, J. Wu, R. Dou, et al., *Opt. Express*, **29**, 12471 (2021).
15. J. Tang, E. Li, F. Wang, et al., *IEEE Photonics J.*, **12**, 1501107 (2020).
16. S. Lamrini, P. Koopmann, M. Schäfer, et al., *Opt. Lett.*, **37**, 515 (2012).
17. E. C. Ji, Q. Liu, X. Z. Cao, et al., *IEEE J. Quantum Electron.*, **52**, 1700208 (2016).
18. X. M. Duan, L. J. Li, Y. J. Shen, and B. Q. Yao, *Appl. Phys. B*, **124**, 1 (2018).
19. X. M. Duan, Y. J. Shen, Z. Zhang, et al., *Infrared Phys. Technol.*, **103**, 103071 (2019).
20. N. P. Barnes, F. Amzajerdian, D. J. Reichle, et al., *Appl. Phys. B*, **103**, 57 (2011).
21. G. A. Newburgh, A. Word-Daniels, A. Michael, et al., *Opt. Express*, **19**, 3604 (2011).
22. V. Jambunathan, X. Mateos, M. C. Pujol, et al., *Appl. Phys. Express*, **4**, 072601 (2011).
23. W. Zhang, Q. Gao, S. Zhou, et al., *Opt. Laser Technol.*, **144**, 107368 (2021).
24. S. Wang, Y. Tang, B. Jiang, et al., *IEEE Photonics Technol. Lett.*, **25**, 2153 (2013).
25. X. Duan, J. Wu, Y. Ding, et al., *Opt. Laser Technol.*, **158**, 108929 (2023).
26. P. Q. Kang, X. L. Zhang, S. Pang, et al., *Opt. Laser Technol.*, **156**, 108525 (2022).
27. X. T. Yang and B. Y. Yao, *Optik*, **125**, 2484 (2014).
28. S. Y. Mi, D. S. Wei, J. W. Tang, et al., *Opt. Laser Technol.*, **152**, 108114 (2022).
29. B. Q. Yao, Y. Ding, X. M. Duan, et al., *Opt. Lett.*, **39**, 4755 (2014).
30. X. M. Duan, W. M. Lin, Y. Ding, et al., *Appl. Phys. B*, **122**, 1 (2016).
31. Y. Ding, T. Liu, and M. Yan, *Appl. Sci.*, **11**, 11537 (2021).
32. J. Wu, Y. Ju, X. Duan, et al., *Infrared Phys. Technol.*, **127**, 104478 (2022).
33. J. Wu, Y. Ju, X. Duan, et al., *Opt. Laser Technol.*, **158**, 108845 (2023).